nature medicine

Autoimmunity and tumor immunity induced by immune responses to mutations in self

Manuel E Engelhorn[1], José A Guevara-Patiño[1], Gabriele Noffz[1], Andrea T Hooper[1,2], Olivia Lou[1,2], Jason S Gold[1], Barry J Kappel[2] & Alan N Houghton[1,2]

Little is known about the consequences of immune recognition of mutated gene products, despite their potential relevance to autoimmunity and tumor immunity. To identify mutations that induce immunity, here we have developed a systematic approach in which combinatorial DNA libraries encoding large numbers of random mutations in two syngeneic tyrosinase-related proteins are used to immunize black mice. We show that the libraries of mutated DNA induce autoimmune hypopigmentation and tumor immunity through cross-recognition of nonmutated gene products. Truncations are present in all immunogenic clones and are sufficient to elicit immunity to self, triggering recognition of normally silent epitopes. Immunity is further enhanced by specific amino acid substitutions that promote T helper cell responses. Thus, presentation of a vast repertoire of antigen variants to the immune system can enhance the generation of adaptive immune responses to self.

Although multicellular organisms have sophisticated machinery to protect their genetic integrity, this machinery is imperfect and errors accumulate in the genome as a consequence of aging and environmental insults. These genetic changes are thought to contribute fundamentally to the pathogenesis of cancer, and genetic instability is accelerated during the processes of malignant transformation and cancer progression[1].

At present, insight into immune recognition of changes in genetic integrity and its consequences is limited. In individual examples, T cells have been shown to recognize mutations expressed by autologous cancer cells[2–12]. Experimental tumors induced by strong mutagens are more immunogenic than are spontaneously arising tumors[13], implying direct recognition of mutations by T cells that prime tumor rejection. Weakly immunogenic tumors, including spontaneous tumors, can be converted to strongly immunogenic tumors by exposure to mutagens[14] and, notably, immunization with mutagenized tumors can induce immunity to the original nonmutagenized tumor, although this secondary immunity is weaker[15]. The basis for this cross-reactive immunity is unclear. Point mutations that alter individual amino acids to create altered peptide ligands with enhanced binding to major histocompatibility complex (MHC) molecules or T-cell antigen receptors can prime T cells against the original, nonmutated peptide, providing one possible explanation[16–18]. Such altered peptide ligands that induce strong responses to poorly or nonimmunogenic antigens have been termed 'heteroclitic epitopes'[19].

Currently, no principles exist for immune recognition of mutated autologous gene products. Here we address this issue through a survey of autoimmunogenic mutations using randomly mutated libraries encoding tissue-specific differentiation antigens. Our results show how mutations can elicit autoimmunity and tumor immunity when expressed in inflammatory environments created during immunization, providing possible molecular links for the known associations of autoimmune diseases with cancer.

RESULTS

Immunity induced by randomly mutated libraries

To investigate how the immune system responds to altered self, complementary DNAs encoding two self proteins were mutated and assessed for immunogenicity. We used melanosome membrane glycoproteins, which determine coat color and are expressed in a tissue-specific manner in melanocytes, as antigens because autoimmunity to these proteins is readily detected by coat hypopigmentation. Injection of vectors encoding syngeneic mouse tyrosinase-related protein 1 (Tyrp1; encoded by *Tyrp1*) and dopachrome tautomerase (Dct, also known as Trp-2; encoded by *Dct*) into C57BL/6 mice induces no detectable immune responses, owing to immune ignorance or tolerance[20–22].

We introduced widespread mutations into the coding sequences of *Tyrp1* and *Dct* cDNAs, using error-prone polymerase chain reaction (PCR)[23], to generate two libraries, each containing $\sim 10^4$ mutagenized clones. Each library had $>150{,}000$ mutations at a frequency of about 1 mutation per 100 nucleotides (**Supplementary Table 1** online), which was predicted to saturate each gene 30-fold with mutations at all codon positions. Individual gene copies had a mean of 15–20 mutations and each copy was predicted to contain a unique set of mutations.

The mutated cDNA libraries were inserted into a eukaryotic expression vector and divided into pools of 2,400 cDNA copies.

[1]Swim Across America Laboratory, Memorial Sloan-Kettering Cancer Center, and [2]Weill Medical and Graduate Schools of Cornell University, 1275 York Avenue, New York, New York 10021, USA. Correspondence should be addressed to A.N.H. (a-houghton@ski.mskcc.org) or M.E.E. (engelho1@mskcc.org).

Received 14 October 2005; accepted 3 January 2006; published online 29 January 2006; doi:10.1038/nm1363

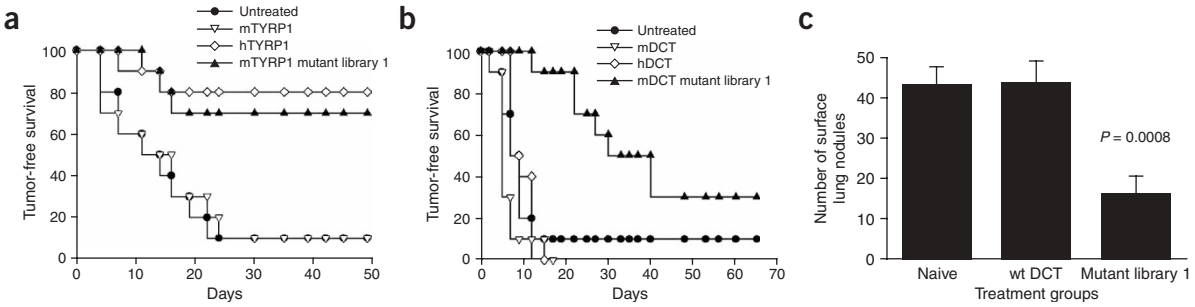

Figure 1 Randomly mutated libraries of *Tyrp1* and *Dct* induce tumor immunity. (**a**,**b**) Kaplan-Meier tumor-free survival curves (15 mice per group) for mutated *Tyrp1* and *Dct* libraries, respectively. Results shown as library 1 are representative of four *Tyrp1* and four *Dct* libraries. (**a**) Mutated mouse *Tyrp1* library 1 significantly improves disease-free survival. Immunization with wild-type *Tyrp1* and that with mutated library 1 were significantly different ($P = 0.007$ by log-rank test). mTYRP1, mouse T*yrp1*; hTYRP1, human *TYRP1*. (**b**) Mutated mouse *Dct* library 1 significantly improves disease-free survival. Immunization with human *DCT* and that with mutated library 1 were significantly different ($P = 0.0056$). (**c**) Effect of treatment with mutated *Dct* library 1. Starting 4 d after intravenous challenge, mice (15 per group) were immunized with a lethal number (10^5) of B16 cells and lungs were evaluated on day 24 after challenge for metastatic lung nodules. The response after immunization with mutated *Dct* library 1 was significantly better than that of the naive and wild-type *Dct* treatment groups. Error bars indicate s.e.m.

Pools were delivered cutaneously by gene gun to C57BL/6 mice[24], and mice were challenged intradermally with a supralethal number of poorly immunogenic B16F10LM3 (B16) melanoma cells and monitored for autoimmune hypopigmentation and tumor rejection. Because B16 melanoma contains nonmutated genomic mouse *Tyrp1* and *Dct* (refs. 25,26; and A.N.H., unpublished data), immunity to these antigens expressed by B16 represents self reactivity.

The DNA pools elicited autoimmunity and tumor rejection. For tumor immunity, the mutated *Dct* library was more potent than the positive control human *DCT* ortholog, and the *Tyrp1* library was comparable to the human *TYRP1* ortholog[20,21] (**Fig. 1a**,**b**). Mice immunized with the *Dct* library in a treatment model in which immunization followed intravenous tumor challenge, as tumors were becoming established in the lungs, rejected tumors (**Fig. 1c**).

Immunization with the mutated *Dct* or *Tyrp1* library induced hypopigmentation. To assess autoimmunity quantitatively, we developed an imaging assay. Digital images of the abdomen were acquired after immunization with wild-type *Tyrp1* or *Dct*, or with the mutated *Tyrp1* or *Dct* library (**Fig. 2a**,**b** and **Table 1**). Hypopigmentation was calibrated with black C57BL/6 (negative control) and white BALB/c (positive control) mice (**Fig. 2a**,**b**). The shift in pixel intensities closely reflected visual scoring of hypopigmentation (**Fig. 2a** and **Table 1**). Histology of hypopigmentation indicated only sparse infiltration of macrophages and occasional lymphoid cells around hair follicles, consistent with little or no inflammatory response, as is observed in established human vitiligo[27,28].

Requirements for CD4$^+$ and CD8$^+$ cells

We have previously shown that diverse immune pathways (such as antibody- and FcR-dependent pathways, and CD8$^+$- and perforin-dependent pathways) lead to identically appearing autoimmunity and tumor immunity[29]. After immunization with the mutated *Dct* library, MHC class I–deficient and MHC class II–deficient mice did not

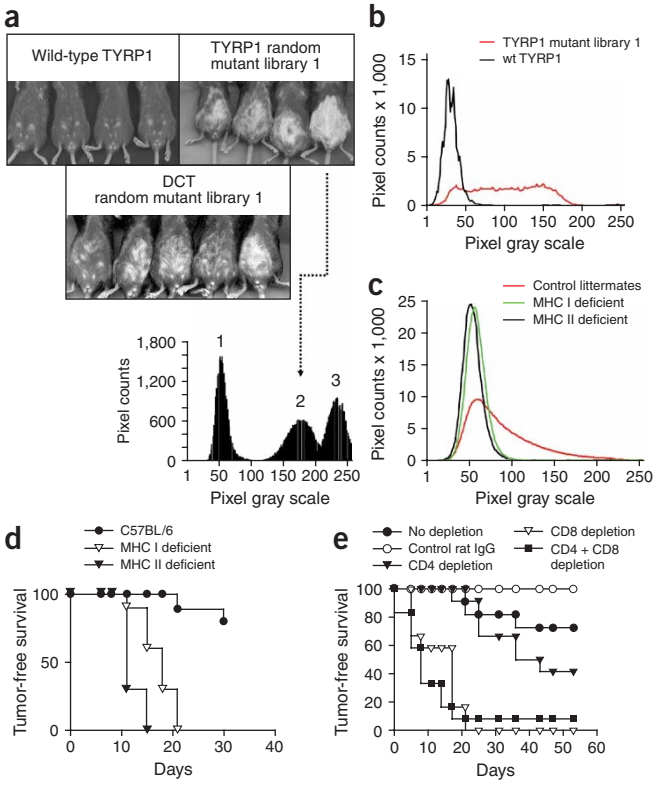

Figure 2 Hypopigmentation upon immunization with mutated *Tyrp1* and *Dct* libraries. (**a**) Hypopigmentation in C57BL/6 mice after the indicated immunizations. Inset, digital pixel population histograms for an untreated C57BL/6 mouse (1), a mouse immunized with mutated *Tyrp1* library 1 (2, arrow) and an untreated BALB/c mouse (3). (**b**) Quantitative digital analysis of autoimmune hypopigmentation induced by randomly mutated *Tyrp1* library 1 as compared with wild-type (wt) *Tyrp1*. All mice from each cohort were analyzed collectively to yield histograms for each group (as in **a**). (**c**) Autoimmunity induced by randomly mutated *Dct* library 1 requires expression of both MHC class I and II. Experimental groups for digital quantification included at least 10 mice per group. (**d**) Tumor protection induced by randomly mutated *Tyrp1* library 1 (15 mice per group) is dependent on expression of MHC class I and II. MHC class I– or II–deficient mice were immunized along with heterozygous control littermates and challenged with B16 melanoma, as in **Figure 1c**. Tumor-free survival curves are shown. (**e**) Tumor rejection induced by mutated *Dct* library 1 (15 mice per group) is abrogated by depleting CD8$^+$ cells or CD4$^+$ plus CD8$^+$ cells with monoclonal antibodies. Depletion of CD4$^+$ cells versus depletion of CD4$^+$ plus CD8$^+$ cells or CD8$^+$ cells was significantly different ($P < 0.0002$ by log-rank test).

Table 1 Induction of autoimmune hypopigmentation

Mouse strain	Immunizing DNA	Number of hypopigmented mice/total	Mean coat pigmentation intensity ± s.d. (digital grayscale units)[a]	Significance[b]
C57BL/6	Control vector	0/28	42.3 ± 4.25	N/A
	wt *DCT*	3/45	46.3 ± 12.0	$P = 1$
	Mutant *DCT* library 1	17/20	57.5 ± 11.2	$P < 0.001$
	Mutant DCT^{M1}	25/43	76.8 ± 40.5	$P < 0.002$
	Mutant $DCT^{M1\text{-}TR}$ (deletion of DCT^{M1} sequence at codon 382)	25/44	69.4 ± 31.2	$P < 0.002$
	wt $DCT^{TR\text{-}382}$ (deletion of wt *DCT* sequence at codon 382)	16/43	62.4 ± 33.4	$P = 0.055$
	Mutant DCT^{M2}	22/34	80.9 ± 42.4	$P < 0.002$
	Mutant $DCT^{M2\text{-}TR}$ (deletion of DCT^{M2} sequence before methionine, at codon 30)	9/10	109.2 ± 38.7	$P < 0.002$
	wt $DCT^{TR\text{-}30}$ (deleting sequence before methionine, at codon 30)	4/10	71.9 ± 37.8	$P < 0.05$
	wt *TYRP1*	2/80	48.0 ± 4.4	N/A[c]
	Mutant *TYRP1* library 1	57/64	102.4 ± 31.0	$P < 0.02$[c]
Littermate controls for MHC deficient	Empty vector	0/14	44.3 ± 4.7	N/A
	Mutant *DCT* library 1	11/15	81.1 ± 25.8	N/A
	Mutant $DCT^{M1\text{-}TR}$	9/15	75.1 ± 21.1	N/A
MHC I deficient	Mutant *DCT* library 1	0/15	51.3 ± 2.8	$P < 0.0002$
	Mutant $DCT^{M1\text{-}TR}$	0/15	53.9 ± 2.4	$P = 0.014$
MHC II deficient	Mutant *DCT library* 1	0/15	48.4 ± 1.8	$P < 0.0002$
	Mutant $DCT^{M1\text{-}TR}$	0/15	51.4 ± 2.6	$P = 0.001$

[a]Mean values of pigmentation on a scale of 1 to 256 (that is, most pigmented to least pigmented) using a digital pixel gray scale. [b]*P* values computed using the Wilcoxon rank sum test, applying the Bonferroni correction for multiple comparisons. For C57BL/6 mice, *P* values were calculated by comparison with control mice mock-immunized with control (empty pCR3 vector). [c]This *P* value not calculated as described; this value was compared to wild-type Tyrp1. For MHC class I– and MHC class II–deficient mice, *P* values were calculated based on the comparison to immunized heterozygous littermates. For information on immunizing DNA, see text, **Figure 3** and **Supplementary Fig. 3** online. wt, wild-type; N/A not applicable.

develop autoimmunity, in contrast to wild-type littermates (**Table 1** and **Fig. 2c**); similar requirements for MHC were observed for tumor immunity induced by the mutated *Tyrp1* library (**Fig. 2d**). The results for the mutated *Tyrp1* library contrast with the antibody-dependent, MHC class I– and $CD8^+$-independent immunity observed after immunization with *TYRP1* ortholog DNA or with recombinant vaccinia virus expressing *Tyrp1* (refs. 28,30). These results indicate that responses from both CD4-expressing ($CD4^+$) and CD8-expressing ($CD8^+$) T cells are required for immunity induced by the mutated libraries.

To determine whether either $CD8^+$ or $CD4^+$ cells are required at the effector phase of immunity, we depleted each cell type individually or together after immunization with the mutated *Dct* library just before B16 melanoma challenge. $CD8^+$ but not $CD4^+$ cells were required at the effector phase (**Fig. 2e**). Because the scoring of hypopigmentation requires weeks to allow regrowth of hairs, it was not possible to distinguish between effector-phase and immunization-phase requirements for $CD4^+$ and $CD8^+$ T cells in the pathogenesis of hypopigmentation. These results with mutated *Tyrp1* and *Dct* suggested the involvement of $CD4^+$ T helper cells for generation of immunity (although not at the effector phase).

Autoimmunity in different MHC backgrounds

Experiments with the mutated *Tyrp1* and *Dct* libraries were extended to B10 congenic strains with H-2^k and H-2^u MHC haplotypes; these strains are distinct from the H-2^b haplotype but have same coat color phenotype as C57BL/6 mice. We observed autoimmune hypopigmentation in both MHC backgrounds (**Supplementary Fig. 1** online). Immunization with human *DCT* and *TYRP1* orthologs induced no autoimmunity (**Supplementary Fig. 1** online and M.E.E., unpublished data). Together, these results show that the MHC allelic restriction imposed by genetic polymorphisms on, for example, the design of individual peptide vaccines can be surmounted by diversity in the mutated libraries.

Identification of immunogenic mutated self antigens

To explore the prevalence of autoimmunogenic mutations, we selected 30 random clones from the mutated *Dct* library, sequenced them completely and individually tested them for immunogenicity. Two mutated clones, termed Dct^{M1} and Dct^{M2}, were immunogenic (**Fig. 3a–c** and **Table 1**). The Dct^{M1} protein has seven amino acid substitutions followed by an in-frame stop codon (T1145A mutation at codon 382; **Fig. 3a**). In Dct^{M2}, a point mutation abrogates the physiological ATG start codon, resulting in two consecutive open reading frames (ORFs): a six-codon out-of-frame ORF spanning nucleotides 15–35, and an in-frame ORF from Met30 to the C terminus of the protein with 16 downstream amino acid substitutions (**Fig. 3a**).

An additional 8 immunogenic clones of mutated *Tyrp1* were detected out of 33 clones isolated from iterative screening of sub-libraries derived from the parent mutated *Tyrp1* library (not selected randomly). One immunogenic clone, $Tyrp1^{M1}$, which induced strong autoimmunity but weak tumor immunity, was analyzed in more detail (**Supplementary Fig. 2** online). Mutated $Tyrp1^{M1}$ had three upstream amino acid substitutions, followed by two nucleotide deletions in codon 113, leading to an altered reading frame of 49 amino acids and a premature stop codon at position 162 (**Supplementary Fig. 2** online).

Two immunogenic mutants were detected in a set of 30 clones randomly picked from the *Dct* library. In addition, all subpools of

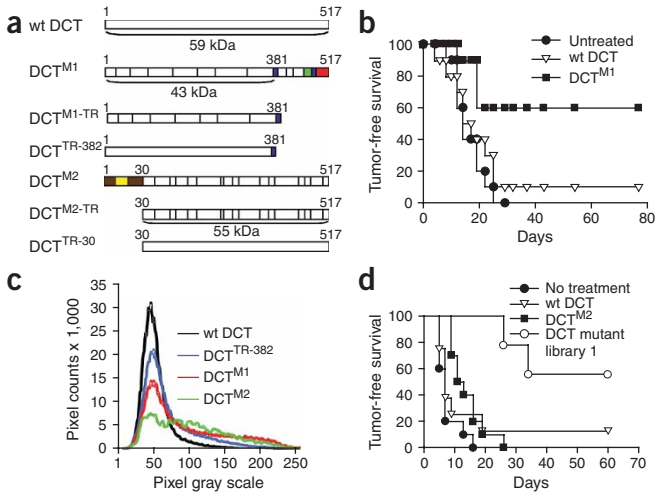

Figure 3 Immunization with Dct and its mutants. (**a**) Wild-type and mutant Dct variants. Numbers at the end of constructs indicate amino acid positions relative to the wild-type sequence; vertical black lines indicate point mutations; blue rectangles indicate stop codons; red box indicates downstream sequence; green box indicates frameshifted segment of Dct^{M1}; brown boxes indicate the N-terminal truncation in Dct^{M2}, which overlaps with a short out-of-frame ORF (yellow box). The predicted relative molecular masses of selected products are shown. (**b**) Tumor immunity induced by Dct^{M1} (15 mice per group). Results from Dct^{M1} and wild-type (wt) *Dct* were statistically different ($P = 0.007$ by log-rank test). (**c**) Hypopigmentation induced by *Dct* variants, measured as in **Figure 2b** (15 mice per group). (**d**) Tumor immunity induced by Dct^{M2} (15 mice per group).

the mutated *Dct* and *Tyrp1* libraries induced equivalent levels of autoimmunity, and sublibraries of the mutated *Tyrp1* library readily yielded immunogenic clones. These observations suggested that there was an abundance of immunogenic variants in the mutated libraries.

All three individual immunogenic mutant clones (Dct^{M1}, Dct^{M2} and $Tyrp1^{M1}$) were characterized by premature stop codons. Because skipping of stop codons and post-translational protein splicing can occur[31,32], we confirmed that the translated products were the predicted truncated polypeptides. *In vitro* translation, carried out with mammalian translation machinery and rabbit reticulocyte preparations, generated polypeptides with the molecular masses predicted for truncated Dct^{M1} and $Tyrp1^{M1}$, and for the second in-frame Dct^{M2} ORF (**Supplementary Fig. 3** online).

Characterization of immunity induced by single mutants

Dct^{M1} elicited both tumor immunity and autoimmunity (**Fig. 3b,c**), and $Tyrp1^{M1}$ produced autoimmunity but minimal tumor immunity (**Supplementary Fig. 2** online). Notably, Dct^{M2} induced autoimmunity but not tumor immunity (**Fig. 3c,d**). Thus, Dct^{M2} segregated autoimmunity to normal follicular melanocytes from immunity to melanoma.

Sequences downstream from the in-frame stop codons of Dct^{M1}, Dct^{M2} and $Tyrp1^{M1}$ had no roles in the induction of autoimmunity because truncated versions of these variants (termed $Dct^{M1\text{-}TR}$, $Dct^{M2\text{-}TR}$ and $Tyrp1^{M1\text{-}TR}$, respectively) retained full immunogenicity (**Table 1** and **Supplementary Fig. 2** online). It seemed possible that the truncations were sufficient to induce autoimmunity. To test this possibility, we engineered a stop codon into wild-type *Dct* corresponding to the stop codon at position 382 in Dct^{M1}, creating $Dct^{TR\text{-}382}$ (**Fig. 3a**). $Dct^{TR\text{-}382}$ induced autoimmunity, albeit less than Dct^{M1} (**Table 1**). Truncated wild-type $Dct^{TR\text{-}30}$, containing a start codon corresponding to the start codon of Dct^{M2} (**Fig. 3a**), also induced hypopigmentation, although less than Dct^{M2} (**Table 1** and **Fig. 3c**). For $Tyrp1^{M1}$, both truncation and the altered reading frame were required for immunity (**Supplementary Fig. 2** online). These results show that nucleotide substitutions leading to either C- or N-terminal truncations can be necessary and sufficient to confer immunity to unaltered self.

Although truncations can be sufficient for autoimmunity, 17 of the 30 randomly chosen mutated *Dct* clones were truncated (without a detectable bias for stop codon position) but did not induce autoimmunity. A comparison between immunogenic and nonimmunogenic clones did not provide any clear distinctions in amino acid substitutions or stop codon positions that accounted for immunogenicity. Overall, these observations show that some truncations in self proteins can elicit autoimmunity. Additional mutations must contribute to autoimmunity because the immunity induced by wild-type truncated Dct proteins was relatively weak.

Altered cellular fates of mutated Dct proteins

We evaluated the fate of products encoded by wild-type *Dct*, $Dct^{M1\text{-}TR}$ and $Dct^{M2\text{-}TR}$ (**Fig. 4** and **Supplementary Fig. 4** online). Constructs

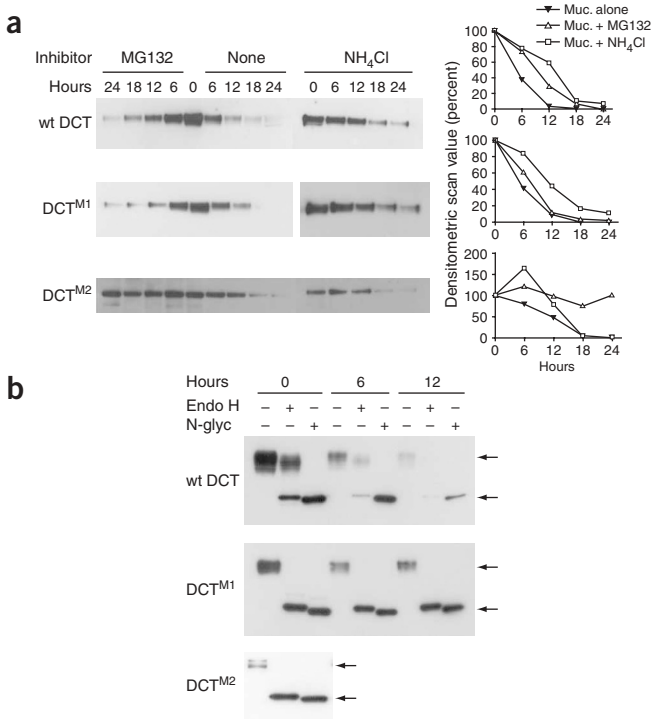

Figure 4 Steady-state stability and glycosylation maturation of Dct and its mutants. (**a**) COS-7 cells were transiently transfected with either Dct or a Dct variant with a C-terminal Flag tag. Translation was stopped 24 h after transfection with muconomycin A. Incubation was then either stopped (0 h) or continued for 6, 12, 18 or 24 h in the presence of the proteasome inhibitor MG132 or ammonium chloride (NH_4Cl) before lysis. Lysates were analyzed by SDS-PAGE followed by immunoblotting. (**b**) COS-7 cells were transiently transfected and translation was stopped as in **a**. Incubation was then stopped (0 h) or continued for 6 or 12 h before lysis. Lysates were either untreated or digested with endoglycosidase H or *N*-glycanase before SDS-PAGE and immunoblot analysis. Upper arrow indicates mature glycoproteins; lower arrow indicates deglycosylated forms Muc, muconomycin A.

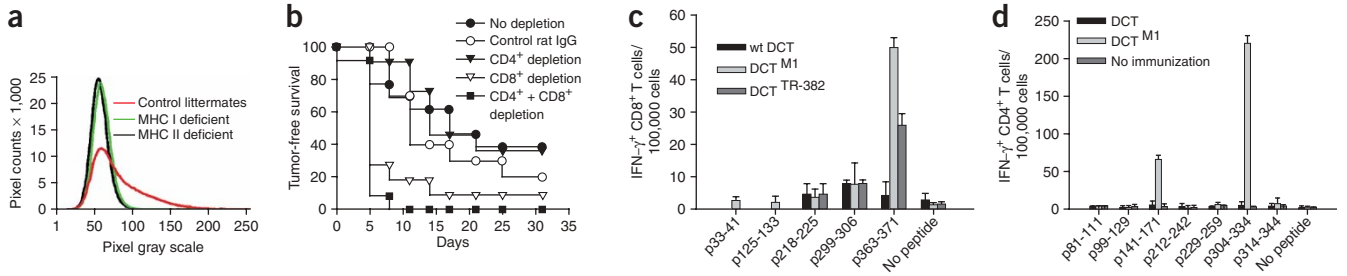

Figure 5 Characterization of immunity induced by Dct^{M1}. (**a**) Autoimmunity induced by Dct^{M1} requires expression of both MHC class I and II. Coat pigmentation was digitally quantified as in **Figure 2b** for 10 mice per group. (**b**) Requirement for CD8$^+$ T cells in tumor immunity induced by Dct^{M1} (15 mice per group). Depletion of CD8$^+$ cells differed significantly from the control rat IgG injection ($P = 0.015$ by log-rank test). (**c**) Splenic CD8$^+$ T cell responses to Dct(363–371) (nonmutated self peptide) of C57BL/6 mice (three mice per group) immunized with wild-type *Dct*, truncated wild-type *Dct* (Dct^{TR}) or Dct^{M1}. Shown are the results of triplicate wells in IFN-γ Elispot assays for predicted wild-type Dct K^b- or D^b-restricted peptides. (**d**) Splenic CD4$^+$ T cell responses to Dct(99–129) and Dct(229–259) of either C57BL/6 mice immunized with wild-type *Dct* or Dct^{M1} or naive mice (three mice per group). Results are from triplicate wells in IFN-γ ELISPOT assays for mutant 31-residue peptides, each spanning a mutation in Dct^{M1} with 15 amino acids upstream and downstream of the mutated residue. (**e**) Test for comparative immunogenicities and cross-reactive responses elicited by wild-type or mutant Dct(304–334). CD4$^+$ T cells from C57BL/6 mice (3 per group) immunized with wild-type Dct(304–334), Dct^{M1}(304–334) or PCC peptide were co-cultured for 40 h with syngeneic splenocytes pulsed with target peptide (wild-type or mutant) at decreasing concentrations (30, 10, 3, 1 and 0.3 μM), as indicated by the triangles. Results are from triplicate wells in an IFN-γ ELISPOT assay. P indicates splenocytes pulsed with PCC peptide. Error bars in **c–e** indicate the s.d.

bearing a Flag tag were transfected into either B78.H1 mouse melanoma cells (a nonpigmented variant of B16) or COS-7 cells. The Flag tag does not alter biosynthesis or stability of the wild-type Dct protein[33]. We did not detect degradation of early post-translational forms of mutant Dct when cells were labeled with [^{35}S]methionine for 5 min and chased for up to 1 h, or any substantial differences in stability when cells were labeled for 20 min and chased for up to 6 h (**Supplementary Fig. 4** online). In addition, when new protein synthesis was inhibited by muconomycin A, the stability of both Dct mutants did not differ substantially from that of wild-type Dct (**Fig. 4a**). Thus, the immunogenicity of the mutated *Dct* clones was not explained simply by increased or decreased instability.

The mutant Dct proteins followed distinct pathways of degradation. The half-lives of both wild-type Dct and mutant Dct^{M1} were prolonged in the presence of ammonium chloride, pointing to degradation in pH-sensitive compartments by endosomal or lysosomal proteases and consistent with the known endosomal sorting of Dct (**Fig. 4a**). Degradation of wild-type Dct was also delayed by the proteasome inhibitor MG132. Notably, degradation of Dct^{M2} was almost completely inhibited by MG132, consistent with cytosolic degradation (**Fig. 4a**). This evidence suggests that Dct^{M1} is processed by endosomal proteases, whereas Dct^{M2} is processed in the cytosol by proteasomes.

The fates of Dct^{M1} and Dct^{M2} differed markedly from that of wild-type Dct. We observed deficient maturation of mutated Dct glycoproteins (**Fig. 4b** and **Supplementary Fig. 4b** online). Carbohydrates of wild-type Dct glycoprotein matured within 20 min, as determined by the resistance of the glycoprotein to endoglycosidase H digestion after a 20-min pulse with [^{35}S]methionine (**Supplementary Fig. 4b** online), indicating that high-mannose asparagine-linked polysaccharides had been modified in the secretory pathway as the protein moved beyond the endoplasmic reticulum (ER) through the Golgi complex. By contrast, both mutant Dct proteins remained sensitive to digestion by endoglycosidase H, consistent with a lack of movement through the Golgi for carbohydrate processing (**Fig. 4b** and **Supplementary Fig. 4b** online).

T-cell requirements for immunity

Both CD4$^+$ and CD8$^+$ T-cell responses were necessary for immunity, because neither MHC class I–deficient nor MHC class II–deficient mice developed autoimmunity or tumor immunity after immunization with Dct^{M1} (**Fig. 5a**), $Tyrp1^{M1}$ (**Supplementary Fig. 5a** online) or Dct^{M2} (**Supplementary Fig. 5b** online). Depletion of T-cell subsets just before tumor challenge and adoptive transfer experiments showed that the effector phase of immunity induced by Dct^{M1} was dependent on CD8$^+$ cells (**Fig. 5b** and **Supplementary Fig. 5c** online). These findings recapitulated our results with the mutated libraries, which showed requirements for both T-cell subsets—specifically CD8$^+$ cells at the effector phase and CD4$^+$ T cells for generating immunity.

CD8$^+$ T-cell responses to a wild-type Dct cryptic epitope

Because the truncations did not account for the full autoimmunogenic potency of Dct^{M1}, Dct^{M2} or $Tyrp1^{M1}$, one or more additional mutations must have further promoted immunity. To address this issue, we examined the roles of other mutations in Dct^{M1} in more detail. First, we searched for candidate MHC class I–restricted mutated epitopes in the Dct^{M1} ORF to identify agonist, altered peptide ligands that might create heteroclitic epitopes. Four peptides, selected by the criterion that the mutation was present in a peptide predicted to bind to K^b or D^b MHC molecules, did not induce recognition of the mutated or corresponding wild-type peptides by CD8$^+$ T cells (data not shown).

Next, five unaltered wild-type Dct peptides containing one or more canonical anchor residues for binding to either K^b or D^b were studied. A previously undefined wild-type D^b-restricted Dct epitope (Dct (363–371); SQVMNLHNL) was recognized by CD8$^+$ T cells from mice immunized with Dct^{M1} and wild-type Dct^{TR-382} but not wild-type *Dct* (**Fig. 5c**). These results show that a normally cryptic, nonmutated MHC class I epitope is immunogenic when processed and presented from truncated (but not full-length) Dct. Truncated wild-type *Dct* (Dct^{TR-382}) was sufficient for inducing T-cell responses to Dct(363–371) (**Fig. 5c**). These results are consistent with the altered cellular fate of Dct^{M1}, which facilitates antigen processing and presentation to create an immunogenic Dct(363–371) epitope.

CD4+ T-cell response to a mutant Dct^{M1} epitope

To screen for mutant MHC class II–restricted epitopes in Dct^{M1}, we assessed CD4+ T-cell responses to 31-residue peptides centered around each mutated residue in the ORF. Two of these peptides (spanning mutations Y156F and L319Q) were recognized by CD4+ T cells expressing interferon (IFN)-γ after immunization with *Dct^{M1}* but not wild-type *Dct* (**Fig. 5d**). CD4+ T cells did not respond to the corresponding wild-type Dct(304–334) peptide, but responded to the L319Q mutant peptide with secretion of IFN-γ and low levels of interleukin (IL)-2 and IL-10 (**Supplementary Fig. 6** online). Amino acids 304–313 were crucial for the immunogenic determinant created by the L319Q mutation, because there was no response to an overlapping 31-residue Dct(314–344) peptide (data not shown). When 31-residue peptides covering positions 304–334 of wild-type Dct and mutant Dct^{M1} were used for immunization, the wild-type peptide elicited no CD4+ response, whereas the mutant peptide induced CD4+ T-cell responses to itself but not the wild-type peptide (**Fig. 5e**).

Competition experiments to assess relative avidities for I-A^b showed that the wild-type Dct peptide bound to I-A^b and the mutant Dct^{M1} peptide did not have substantially greater binding (**Supplementary Fig. 5** online). Further inspection of Dct(304–334) identified a canonical nonameric peptide, EKLPTLKNV, with anchor residues for binding to I-A^b forming a core sequence for an extended MHC class II–restricted peptide[34]. The mutant peptide EKQPTLKNV (with an L to Q mutation) is predicted to show the same MHC class II affinity as the wild-type EKLPTLKNV peptide. The glutamine residue of the mutated EKQPTLKNV peptide–I-A^b complex is predicted to point in the solvent phase toward the T-cell antigen receptor, away from the MHC, on the basis of the structure of I-A^b and the sequences of peptides known to bind I-A^b (ref. 34). These observations provide an explanation for why MHC class II molecules are required in priming immunity by the *Dct^{M1}* mutant and why the mutant is a stronger immunogen than truncated wild-type *Dct^{TR}*. Immunogenicity is probably due to enhanced avidity of specific T-cell receptors for the mutant peptide bound to MHC class II molecules, with no cross-reactivity to wild-type Dct. Together, these results indicate that a mutation in *Dct^{M1}* creates an MHC class II–restricted neoepitope that generates CD4+ T helper cells.

DISCUSSION

Our results support the idea that the adaptive immune system can recognize and respond to changes in genomic integrity. The potential benefit of such a function is evident because mutations, which accumulate with aging and with chronic inflammation, have the potential to contribute to the pathogenesis of diseases such as cancer[1]. Such a role for the immune system must be balanced, however, by the necessity to avoid autoimmunity.

Initially, we expected to identify mutations that create rare, agonist, altered peptide ligands, as in the mutated heteroclitic epitopes of the melanosomal proteins gp100 and Tyrp1 (refs. 17,35). We surmised that these epitopes would induce CD8+ T-cell responses that mediate tumor immunity and autoimmunity. Unexpectedly, no such events were detected. Rather, autoimmunity stemmed from an accumulation of individual, weakly autoimmunogenic mutations that altered protein fate, created helper epitopes and induced recognition of nonmutated cryptic epitopes. Truncations were a common feature underlying the autoimmunogenic cDNAs in our survey, including in two additional incompletely analyzed *Tyrp1* clones not presented here (G.N., M.E.E. and A.N.H., unpublished data), for a total of five truncated autoimmunogenic clones. Our observations suggest that inappropriately truncated self proteins can provoke autoimmunity, for example, when expressed in acute inflammatory environments.

Although our experimental system is an imperfect emulation of the progressive accumulation of somatic mutations over time, it supports the notion that accumulated mutations have a role in the pathogenesis of autoimmunity. This hypothesis represents an alternative, not mutually exclusive, mechanism to other proposed pathogenic events for autoimmunity involving microbial infections with cross-reactivity to self (antigen mimicry).

Our results show that immunogenic mutations in tissue-specific self proteins can be readily detected. These observations permit us to estimate a threshold number of mutations that accumulate before autoimmunity is observed. Out of 30 clones containing a total of 477 mutations, 2 were auto-immunogenic (one immunogenic protein per 239 mutations). Whether spontaneous autoimmune diseases are induced by immune reactivity to mutated self proteins remains to be seen. An implication of these observations is that autoimmunity could be elicited by normal or transformed somatic cells carrying a high density of mutations, perhaps promoted by adjuvant effects of acute local inflammation. Mutations in somatic cells, related to the high but imperfect fidelity of mammalian DNA replication, would generate numerous mutations in progeny cells, with the location and concentration of mutant progeny depending on when the mutations occurred during differentiation. Because somatic mutations accumulate with age, limitations in T-cell repertoire and T helper cell deficiencies that occur with aging could balance an otherwise increased risk of autoimmunity.

Because we used autoimmunity as the readout in our screen for immunogenic mutations, we identified only mutations that induce self-reactivity. Autoimmunity is not, however, a requisite for immunity to cancer. Mutations that lead to recognition of mutated epitopes presented only by cancer cells without cross-recognition of the corresponding native epitopes may be particularly important for cancer immunity, as suggested by the robust immunogenicity of mouse tumors induced by strong mutagens. Consequently, the threshold for immunogenic mutations in our experiments probably underestimates the frequency of directly immunogenic mutations. Our current work addresses the direct immunogenicity of mutated self.

Here we analyzed selected individual immunogenic mutants. The truncation in *Dct^{M1}* was sufficient for inducing immune responses to a cryptic, nonmutated MHC class I–restricted epitope. Clues to the basis for recognition of this epitope come from the altered fate and deficient maturation of Dct^{M1}, which support a trafficking pathway in which the mutated protein moves from the ER to endocytic compartments for degradation, bypassing processing in the Golgi. Dct^{M1} peptides generated in the endocytic pathway might access MHC class I molecules by retrotransport to the ER or translocation to the cytosol and then to the ER. This altered fate must contribute to presentation of this normally cryptic epitope. Immunogenicity of *Dct^{M1}* is further enhanced by an additional point mutation that creates a new MHC II helper epitope without inducing cross-reactive responses to the corresponding native peptide.

We identified two other mutants (*Dct^{M2}* and *Tyrp1^{M1}*) that elicited autoimmunity but little or no detectable tumor immunity. We previously reported that effector mechanisms of autoimmunity uncouple from those of tumor immunity after immunization with the human *DCT* ortholog[36]. We suspect that uncoupling reflects, in part, differences in the milieu of normal melanocytes versus malignant melanocytes in invasive tumors, as well as intrinsic

differences between normal and malignant melanocytes. Mouse melanocytes are located in hair follicles, where they are surrounded by an orderly environment constrained by a basement membrane, and show strict control of growth during the hair cycle. Melanocyte stem cells and their progeny express Dct, so perhaps autoimmunity to Dct targets stem cells. Invasive melanoma cells are motile, proliferating cells that are less constrained by signals from stroma and neighboring normal cells. Melanoma cells express transforming growth factor-β and other molecules that promote immune evasion and often have altered antigen-processing machinery. In addition, we speculate that the range of epitopes presented by B16 melanoma differs from that presented by healthy melanocytes. For example, mRNA splicing patterns diverge between melanoma (including B16) and normal melanocytes[37,38]. Melanomas and melanocytes therefore probably present overlapping but distinct repertoires of epitopes.

From the perspective of vaccine design, specific mutations may give rise to antagonist peptide ligands that inhibit T-cell responses. Thus, mutated libraries may contain antagonist epitopes, and their enrichment might be beneficial for autoimmunity. In our libraries, however, the balance favored agonist ligands because autoimmunity was observed for all library pools. Mutated libraries were at least as potent as orthologs and were immunogenic in hosts with different MHC haplotypes. The diversity of mutations in a library provides numerous peptides with potential for binding to several MHC alleles (~800 MHC class I and ~600 MHC class II alleles in humans[39]), bypassing the need to identify and to validate epitopes for individual alleles. These findings suggest that mutated libraries may be an alternative to peptide-based vaccines, which are limited by MHC polymorphisms.

We propose that mutated DNA libraries might be effective against pathogens that escape immune attack through high mutation rates or other mechanisms that generate antigenic variants. For example, mutations abolishing dominant epitopes lead to immune escape for HIV. Although escape variants for individual epitopes cannot be prevented, other mutations in pathogens could create new epitopes. A mutated DNA library vaccine could broaden the specificities of T-cell responses to increase the probability of recognizing mutated epitopes, without requiring prior knowledge of their identity. In addition, vaccines are less efficient in the aging population[40]. Decreased diversity of the T-cell repertoire is a hallmark of age-related immunodeficiency. One strategy to make the best of a restricted repertoire is to activate T-cell receptors recognizing subdominant epitopes of pathogens, a situation with some similarities to the induction of immunity to subdominant or cryptic epitopes expressed by cancer. The strategy of mutated DNA vaccines has the potential to address limitations of vaccination aganist cancer and infectious pathogens by generating broad repertoires of altered antigens.

METHODS

Mice. We used the following female mice (aged 8–10 weeks): C57BL/6 (US National Cancer Institute); B10.BR-H2^{k} H2-T18^{a}/SgSnJ and B10.PL-H2^{u} H2-T18^{a} (73NS)/Sn B6 RAG1 (Jackson Laboratories); and MHC class I deficient (B2MN5-M) and class II deficient (ABBN5-M), and controls (B2MN6-W; all from Taconic Farms). Care of mice followed institutional guidelines under a protocol approved by the Institutional Animal Care and Use Committee at Memorial Sloan-Kettering Cancer Center.

Plasmid constructs. We subcloned mouse *Tyrp1* and human *TYRP1* cDNAs into a WRG7077BEN eukaryotic expression vector[41]. We generated PCR products encoding mutant or wild-type Tyrp1 with the primers 5′-TTGCGGCCGCCATGAAATCTTACAACGTG-3′ and 5′-CGGAATTCTCAGACCATGGAGTGGTTA-3′, and subcloned them into vectors at *Not*I and *Eco*RI restriction sites (underlined). Human *DCT* cDNA[21] from N. Restifo (US National Cancer Institute) was cloned into pWRG7077BEN. PCR products encoding mutant or wild-type Dct (upstream primer, 5′-AAGGCGCGCCATGGGCCTTGTGGGATG-3′; downstream primer, 5′-ATGCGGCCGCTAGGCTTCCTCCGTGTA-3′) were subcloned into pWRGANEB (pWRG7077BEN variant) at *Asc*I and *Not*I sites (underlined). We created pWRGANEB by inserting an oligonucleotide duplex (5′-GGCCTGGCGCGCCGTACGTTAACATCGATGC-3′ and 5′-GGCCGCATCGATGTTAACGTACGGCGCGCCA-3′) into the *Not*I site of pWRG7077BEN. We created 3′-truncated cDNA inserts encoding wild-type Dct and Dct^{M1} by PCR using the same upstream oligonucleotide and a second downstream oligonucleotide (5′-ATGCGGCCGC*TA*GGCATTGGTCCCATTCAGGAAG-3′; the *Not*I site is underlined and stop codon in the antisense strand is italicized). We created a 5′-truncated cDNA encoding Dct^{M2} by PCR using the above downstream oligonucleotide and a second upstream oligonucleotide (5′-AAGGCGCGCCATGACCTTGGATGGCGTGCTG-3′). Wild-type and Dct^{M1} with a Flag epitope at the C terminus were constructed by inserting the cDNAs between the *Eco*RV and *Sal*I sites in pCMV-Tag 4A (Stratagene). Fragments were reamplified to create an in-frame Flag epitope (wild-type, 5′-ATTCATAGTCGACGGCTTCCTCCGTGTATCTCTTG-3′; Dct^{M1}, 5′-ATTCATAGTCGACGGCATTGGTCCCATTCAGGAAG-3′).

Random PCR mutagenesis and creation of libraries. We carried out random mutagenesis using previously described conditions[23]. Independent *Escherichia coli* transformants containing subcloned mutagenized PCR products were plated at 800–1,000 colonies per 100-mm plate. We used either an indexed library protocol, in which 2,400 clones were individually chosen, arrayed in 96-well plates and replicated using a Boekel replicator tool (Fisher Scientific), or a batch protocol, in which the original 100-mm plate was replica-plated twice. For selection of individual *Tyrp1* clones, we chose 2,500 clones and arrayed them in 96-well plates. We identified immunogenic clones through reiterative *in vivo* screening of pools representing rows and columns of the indexed arrays. Colonies were expanded and plasmid DNA was extracted (Qiagen).

Immunization and tumor challenge. We prepared DNA for immunization as previously described[41]. Mice were depilated and immunized with gold particles coated in DNA (4 μg per mouse) by an Accell helium-pressured gene gun (PowderJect Vaccines) usually four to five times weekly. For tumor therapy experiments, mice were immunized every fourth day, starting 4 d after intravenous inoculation of 10^5 B16 cells, and killed on day 24. Five days after the last immunization, we challenged mice intradermally with 10^5 B16 melanoma cells. Depletion of CD4$^+$ and CD8$^+$ T cells was done by weekly intraperitoneal injections of 0.5 mg of GK1.5 and 53.6-72 rat monoclonal antibodies, respectively. Depletion (>90%) started 3 d before tumor challenge and was confirmed by FACS analysis of peripheral blood. C57BL/6 donor mice were immunized four times and were killed 5 d after the last boost. We then transferred purified CD4$^+$ or CD8$^+$ splenocytes into B6 *Rag1*$^{-/-}$ mice at a 1/1 donor/recipient ratio. We intradermally challenged recipients the next day with 50,000 B16 melanoma cells.

***In vitro* transcription and translation assays.** We used the cytomegalovirus-based plasmids for immunization as templates for *in vitro* transcription and translation with rabbit reticulocyte lysates (Promega). We used biosynthetic labeling with [^{35}S]methionine to detect newly synthesized polypeptides. We analyzed reactions by SDS-PAGE and autoradiography.

Peptide sequences. We used the following peptides (Genemed Synthesis) for T-cell assays and/or immunization. For D^{b}-restricted peptides: Dct(33–41) (DGVLNKECC), Dct(125–133) (ILRRNIHSL) and Dct(363–371) (SQVMNLHNL). For K^{b}-restricted peptides: Dct(218–225) (TWHRYHLL) and Dct(299–306) (CNGTYEGL). For I-A^{b}–restricted peptides: Dct(81–111) (DDREQWPRKFFNRTCECTGNFAGYNCGGCKF), Dct(99–129) (GNFAGYNCGGCKFGWSGPDCNRKKPAILRRN), Dct(141–171) (FLGALDLAKKSIHPDFVITTQHWLGLLGPNG), Dct(212–242) (QGPAFVTWHRYHLLWQERELQRLTGNESFAL), Dct(229–259) (RELQRLTGNESFALPSWNFATGKNECDV CTD),

Dct(304–334) (EGLLRRNKVGRNNEKQPTLKNVQDCQ SLQKF) and Dct(314–344) (RNNEKQPTLKNVQDCQSLQKFDSPPFFQNST); in each case the mutated amino acid is underlined. We evaluated the predicted affinity of D^b- and K^b-restricted peptides with the Syfpeithi database. We predicted I-A^b binding with the Rankpep database. The pigeon cytochrome *c* and chicken ovalbumin I-A^b–binding positive control peptides were PCC(43–58) (AEGFSYTDANKNKGIT) and OVA(323–339) (ISQAVHAAHAEINEAGR).

ELISPOT assays were done as previously described[42] using purified $CD4^+$ and $CD8^+$ lymphocytes (MACS system, Miltenyi Biotech). Mouse IFN-γ–specific capture and detection antibodies (AN18 and biotinylated R4-6A2) were from Diapharma. For $CD8^+$ lymphocytes, the targets were EL4 lymphoma cells preincubated with 10 μg/ml of peptide; for $CD4^+$ lymphocytes, the targets were naive syngeneic splenocytes pulsed with 10 μg/ml of peptide. We coincubated targets (10^4) for 20 h at 37 °C. Spots were developed with streptavidin-conjugated horseradish peroxidase.

Endoglycosidase H and immunoblot analysis. We transfected B78H1 melanoma cells (a *Tyrp1*- and *Dct*-negative line derived from B16) or COS-7 cells with constructs encoding Flag-tagged wild-type, Dct^{M1} or Dct^{M2} using Lipofectamine 2000 (Invitrogen). At 48 h, we labeled cells (for 5 or 20 min) with 50 μCi/ml of [^{35}S]methionine (Protein Express, DuPont NEN) and lysed them immediately or after chasing. We immunoprecipitated lysates with an agarose-prebound Flag-specific antibody (Sigma) and treated portions of lysates for 8 h with 0.005 units of endoglycosidase H or *N*-glycanase (Sigma) before SDS-PAGE analysis. We determined the proportion of endoglycosidase H–sensitive material by densitometry using ScionImage software (Scion). Alternatively, we directly lysed transfected COS-7 cells and analyzed them by SDS-PAGE and western blotting using a horseradish peroxidase–conjugated Flag-specific antibody (Sigma) after normalizing gel loading for equivalent total protein content.

Quantification of autoimmune hypopigmentation. Mouse abdomens were scanned with a Hewlett-Packard Series 650 scanner and HP PrecisionScanPro software (highlights, 255; shadows, 0; midtones, 2.2; resolution, 150). We made image adjustments using Adobe Photoshop such that pixel populations from C57BL/6 and a BALB/c mice were separated on the 1–256 gray scale without being compressed against the lower or upper limits (contrast: +15; level parameters: 40, 1, 255). We quantified the area of hair regrowth using ScionImage software. The corresponding pixel population was scored on the 1–256 gray scale. Experimental groups for digital quantification contained ≥10 mice.

Statistical analysis. Tumor-free survival was plotted by Kaplan-Meier plots and significance was assessed by log-rank analysis. For analysis of hypopigmentation, groups were compared using the Wilcoxon rank sum test with Bonferroni correction for multiple comparisons.

URLs. Syfpeithi database, http://www.syfpeithi.de.
Rankpep database, http://mif.dfci.harvard.edu/Tools/rankpep.html.

Note: Supplementary information is available on the Nature Medicine website.

ACKNOWLEDGMENTS

We thank S. Tiwari for technical assistance; R. Stan for help in editing the manuscript; K. Panageas for help with statistical analysis; and V. Setulari and D. Posnett for comments and discussions. This work was supported by the US National Cancer Institute (grants CA56821, CA33049 and CA59350 to A.N.H.), Swim Across America, the Peter Jay Sharp and the Breast Cancer Research Foundations, the Annenberg Hazen Award, the TJ Martell Foundation, the Lymphoma Foundation, Mr. William H. Goodwin and Mrs. Alice Goodwin, and the Commonwealth Cancer Foundation for Research, the Experimental Therapeutics Center of Memorial Sloan-Kettering Cancer Center and the Louis and Anne Abrons Foundation. M.E.E. was supported by postdoctoral fellowships from the Swiss National Fund for Scientific Research (81GE-53218) and the Cancer Research Institute, New York.

COMPETING INTERESTS STATEMENT

The authors declare that they have no competing financial interests.

Published online at http://www.nature.com/naturemedicine/
Reprints and permissions information is available online at http://npg.nature.com/reprintsandpermissions/

1. Hahn, W.C. & Weinberg, R.A. Rules for making human tumor cells. *N. Engl. J. Med.* **347**, 1593–1603 (2002).
2. Mandruzzato, S., Brasseur, F., Andry, G., Boon, T. & van der Bruggen, P.A. CASP-8 mutation recognized by cytolytic T lymphocytes on a human head and neck carcinoma. *J. Exp. Med.* **186**, 785–793 (1997).
3. Coulie, P.G. *et al.* A mutated intron sequence codes for an antigenic peptide recognized by cytolytic T lymphocytes on a human melanoma. *Proc. Natl. Acad. Sci. USA* **92**, 7976–7980 (1995).
4. Robbins, P.F. *et al.* A mutated β-catenin gene encodes a melanoma-specific antigen recognized by tumor infiltrating lymphocytes. *J. Exp. Med.* **183**, 1185–1192 (1996).
5. Wang, R.F., Wang, X., Atwood, A.C., Topalian, S.L. & Rosenberg, S.A. Cloning genes encoding MHC class II–restricted antigens: mutated CDC27 as a tumor antigen. *Science* **284**, 1351–1354 (1999).
6. Wang, R.F., Parkhurst, M.R., Kawakami, Y., Robbins, P.F. & Rosenberg, S.A. Utilization of an alternative open reading frame of a normal gene in generating a novel human cancer antigen. *J. Exp. Med.* **183**, 1131–1140 (1996).
7. Zorn, E. & Hercend, T. A natural cytotoxic T cell response in a spontaneously regressing human melanoma targets a neoantigen resulting from a somatic point mutation. *Eur. J. Immunol.* **29**, 592–601 (1999).
8. Wolfel, T. *et al.* A p16INK4a-insensitive CDK4 mutant targeted by cytolytic T lymphocytes in a human melanoma. *Science* **269**, 1281–1284 (1995).
9. Hogan, K.T. *et al.* The peptide recognized by HLA-A68.2–restricted, squamous cell carcinoma of the lung-specific cytotoxic T lymphocytes is derived from a mutated elongation factor 2 gene. *Cancer Res.* **58**, 5144–5150 (1998).
10. Gaudin, C., Kremer, F., Angevin, E., Scott, V. & Triebel, F. A hsp70–2 mutation recognized by CTL on a human renal cell carcinoma. *J. Immunol.* **162**, 1730–1738 (1999).
11. Chiari, R. *et al.* Two antigens recognized by autologous cytolytic T lymphocytes on a melanoma result from a single point mutation in an essential housekeeping gene. *Cancer Res.* **59**, 5785–5792 (1999).
12. Brandle, D., Brasseur, F., Weynants, P., Boon, T. & Van den Eynde, B. A mutated HLA-A2 molecule recognized by autologous cytotoxic T lymphocytes on a human renal cell carcinoma. *J. Exp. Med.* **183**, 2501–2508 (1996).
13. Prehn, R.T. & Main, J.M. Immunity to methylcholanthrene-induced sarcomas. *J. Natl. Cancer Inst.* **18**, 769–778 (1957).
14. Boon, T. & Kellermann, O. Rejection by syngeneic mice of cell variants obtained by mutagenesis of a malignant teratocarcinoma cell line. *Proc. Natl. Acad. Sci. USA* **74**, 272–275 (1977).
15. Boon, T. & Van Pel, A. Teratocarcinoma cell variants rejected by syngeneic mice: protection of mice immunized with these variants against other variants and against the original malignant cell line. *Proc. Natl. Acad. Sci. USA* **75**, 1519–1523 (1978).
16. Slansky, E.J. *et al.* Enhanced antigen-specific antitumor immunity with altered peptide ligands that stabilize the MHC-peptide-TCR complex. *Immunity* **13**, 529–538 (2000).
17. Dyall, R. *et al.* Heteroclitic immunization induces tumor immunity. *J. Exp. Med.* **188**, 1553–1561 (1998).
18. Gold, J.S. *et al.* A single heteroclitic epitope determines cancer immunity following xenogeneic DNA immunization against a tumor differentiation antigen. *J. Immunol.* **170**, 5188–5194 (2003).
19. Makela, O. Single lymph node cells producing heteroclitic bacteriophage antibody. *J. Immunol.* **95**, 378–386 (1965).
20. Weber, L.W. *et al.* Tumor immunity and autoimmunity induced by immunization with homologous DNA. *J. Clin. Invest.* **102**, 1258–1264 (1998).
21. Bowne, W.B. *et al.* Coupling and uncoupling of tumor immunity and autoimmunity. *J. Exp. Med.* **190**, 1717–1722 (1999).
22. Leitner, W.W. *et al.* Alphavirus-based DNA vaccine breaks immunological tolerance by activating innate antiviral pathways. *Nat. Med.* **9**, 33–39 (2003).
23. Cadwell, R.C. & Joyce, G.F. Mutagenic PCR. *PCR Methods Appl.* **3**, S136–S140 (1994).
24. Barry, M.A., Lai, W.C. & Johnston, S.A. Protection against mycoplasma infection using expression-library immunization. *Nature* **377**, 632–635 (1995).
25. Shibahara, S. *et al.* Cloning and expression of cDNA encoding mouse tyrosinase. *Nucleic Acids Res.* **14**, 2413–2427 (1986).
26. Jackson, I.J. *et al.* A second tyrosinase-related protein, TRP-2, maps to and is mutated at the mouse slaty locus. *EMBO J.* **11**, 527–535 (1992).
27. Hara, I., Takechi, Y. & Houghton, A.N. Implicating a role for immune recognition of self in tumor rejection: passive immunization against the brown locus protein. *J. Exp. Med.* **182**, 1609–1614 (1995).
28. Overwijk, W.W. *et al.* Vaccination with a recombinant vaccinia virus encoding a 'self' antigen induces autoimmune vitiligo and tumor cell destruction in mice: Requirement for $CD4^+$ T lymphocytes. *Proc. Natl. Acad. Sci. USA* **96**, 2982–2987 (1999).
29. Turk, M.J., Wolchok, J.D., Guevara-Patino, J.A., Goldberg, S.M. & Houghton, A.N. Multiple pathways to tumor immunity and concomitant autoimmunity. *Immunol. Rev.* **188**, 122–135 (2002).
30. Weber, L.W. *et al.* Tumor immunity and autoimmunity induced by immunization with homologous DNA. *J. Clin. Invest.* **102**, 1258–1264 (1998).

31. Hanada, K., Yewdell, J.W. & Yang, J.C. Immune recognition of a human renal cancer antigen through post-translational protein splicing. *Nature* **427**, 252–256 (2004).
32. Vigneron, N. *et al.* An antigenic peptide produced by peptide splicing in the proteasome. *Science* **304**, 587–590 (2004).
33. Negroiu, G., Dwek, R.A. & Petrescu, S.M. Tyrosinase-related protein-2 and -1 are trafficked on distinct routes in B16 melanoma cells. *Biochem. Biophys. Res. Commun.* **328**, 914–921 (2005).
34. Zhu, Y., Rudensky, A.Y., Corper, A.L., Teyton, L. & Wilson, I.A. Crystal structure of MHC class II I-Ab in complex with a human CLIP peptide: prediction of an I-Ab peptide-binding motif. *J. Mol. Biol.* **326**, 1157–1174 (2003).
35. Restifo, N.P., Spiess, P.J., Karp, S.E., Mule, J.J. & Rosenberg, S.A. A nonimmunogenic sarcoma transduced with the cDNA for interferon γ elicits $CD8^+$ T cells against the wild-type tumor: Correlation with antigen presentation capability. *J. Exp. Med.* **175**, 1423–1431 (1992).
36. Bowne, W.B. *et al.* Coupling and uncoupling of tumor immunity and autoimmunity. *J. Exp. Med.* **190**, 1717–1722 (1999).
37. Le Fur, N., Kelsall, S.R., Silvers, W.K. & Mintz, B. Selective increase in specific alternative splice variants of tyrosinase in murine melanomas: a projected basis for immunotherapy. *Proc. Natl. Acad. Sci. USA* **94**, 5332–5337 (1997).
38. Watahiki, A. *et al.* Libraries enriched for alternatively spliced exons reveal splicing patterns in melanocytes and melanomas. *Nat. Methods* **1**, 233–239 (2004).
39. Robinson, J. *et al.* IMGT/HLA and IMGT/MHC: sequence databases for the study of the major histocompatibility complex. *Nucleic Acids Res.* **31**, 311–314 (2003).
40. Effros, R.B. Problems and solutions to the development of vaccines in the elderly. *Immunol. Allergy Clin. North Am.* **23**, 41–55 (2003).
41. Ross, H.M. *et al.* Priming for T-cell-mediated rejection of established tumors by cutaneous DNA immunization. *Clin. Cancer Res.* **3**, 2191–2196 (1997).
42. Lewis, J.J. *et al.* Evaluation of $CD8^+$ T-cell frequencies by the Elispot assay in healthy individuals and in patients with metastatic melanoma immunized with tyrosinase peptide. *Int. J. Cancer* **87**, 391–398 (2000).